Article

Microprobe-XRF Assessment of Nutrient Distribution in Soybean, Cowpea, and Kidney Bean Seeds: A Fabaceae Family Case Study

Gabriel Sgarbiero Montanha, Sara Luiza Zachi Romeu, João Paulo Rodrigues Marques, Lívia Araújo Rohr, Eduardo de Almeida, André Rodrigues dos Reis, Francisco Scaglia Linhares, Sabrina Sabatini, and Hudson Wallace Pereira de Carvalho*

Read Online

ACCESS | Metrics & More | Article Recommendations | Supporting Information

ABSTRACT: The present study explored microprobe X-ray fluorescence (XRF) spectroscopy for quantitative and space-resolved distribution of macro, i.e., potassium (K), phosphorus (P), sulfur (S), and calcium (Ca), and micronutrients, i.e., iron (Fe), zinc (Zn), and manganese (Mn) elemental composition in the cross-sectioned seeds of cowpea (*Vigna unguiculata* L.), kidney bean (*Phaseolus vulgaris* L.), and soybean (*Glycine max* L.) seeds, which are important agricultural species within the Fabaceae family. It unveils that both macro and micronutrients were heterogeneously distributed across seed tissues. Most of the P and S, Fe, Zn, and Mn were mainly found at the embryo axis tissues in all three Fabaceae species, whereas K was spread along the cotyledon and Ca was mostly observed trapped at the seed coat region. Furthermore, the Pearson correlation coefficient revealed a strong spatial correlation between P and S, and K and S in cowpea and soybean seed tissues, whereas Zn and Mn association was also recorded. Therefore, the μ-XRF technique is an important tool for assessing seed nutrient distribution, thus subsidizing the physiological role of nutrients in seeds and fostering innovative approaches for nutrient supply and biofortification.

KEYWORDS: μ-XRF, nutrients, seeds, cowpea, soybean, kidney bean

1. INTRODUCTION

The Fabaceae (Leguminosae) is the third largest family of flowering plants,[1] encompassing ca. 800 genera and 20 000 described species,[2] some of which are important species for livestock feed and human food, such as peanuts (*Arachis hypogaea*), peas (*Pisum sativum*), common bean (*Phaseolus vulgaris*), chickpea (*Cicer arietinum*), cowpea (*Vigna unguiculata*), lentil (*Lens culinaris*), and soybean (*Glycine max* (L.) Merrill). Notably, legume seeds are a remarkable source of carbohydrates, proteins, and oil.[3,4] Only soybean seeds account for more than 1:2 of the seed-based oil and 2:3 of all of the protein meals currently produced worldwide.[5]

Besides macromolecules, i.e., protein, oil, and carbohydrates, the mineral nutrients stowed in the seed tissues are also crucial either as structural or cofactors of proteins, such as enzymes and transcription factors involved in the myriad of biochemical processes taking place during germination and early seedling development stages.[6,7] Although seeds are expected to safeguard their reserves at suitable levels prior to germination,[8] one should notice that these figures might be affected by environmental conditions and crop management practices.[9,10] In this regard, the mineral composition of seeds has been widely investigated aiming at understanding whether it affects the development of plants under nonoptimal conditions, e.g., drought or salinity-induced stress, as well as exploring potential strategies for boosting its nutritional quality.[7,11−13]

On the other hand, space-resolved nutrient localization revealed that nutrient distribution varies across seed tissues. Particularly, phosphorus (P), sulfur (S), and potassium (Ca) were mainly found in the embryonic regions, whereas Ca was

found in seed coat and hilum regions of *Crotalaria ochroleuca* and *Arabidopsis thaliana* seeds,[14,15] whereas beneficial elements, such as selenium (Se) and nickel (Ni), respectively, can be found in the embryo and cotyledon tissues of cowpea (*V. unguiculata* L.), buckwheat (*Fagopyrum esculentum*), and soybean (*G. max* (L.) Merrill).[16−18] These few studies lead to the following question: How preserved is this spatial pattern across Families and within Families?

Despite the importance of characterizing the nutrient distribution of the seeds to properly understand the mechanisms underlying their physiology,[19] it is worth highlighting that due to the scarce laboratory-based microanalysis approaches, the nutrient studies in leguminous seeds commonly rely on bulk analyses, i.e., relating only to their total content. In this context, microprobe X-ray fluorescence (μ-XRF) spectroscopy stands out as a suitable analytical technique for studying the nutrient composition and distribution of biological sample materials, including seeds[15,19−22] under *vivo* conditions or with minimal sample preparation.[22−25]

Previous studies explored the μ-XRF to uncover the elemental distribution in developing soybean seeds and assess
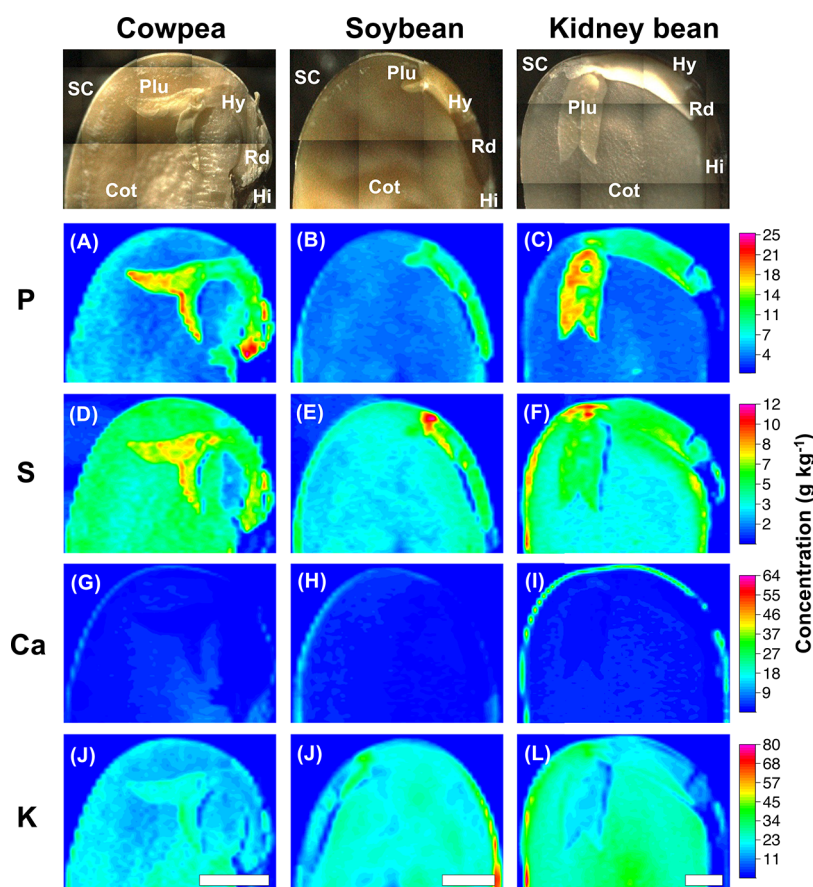
A

Figure 1. Quantitative XRF maps revealing the distribution of P (A−C), S (D−F), Ca (G−I), and K (J−L) in cowpea, soybean, and kidney bean seed cross sections. The concentrations were determined through external cellulose-based calibration curves. SC: seed coat; Cot: cotyledon; Plu: plumule; Hy: hypocotyl; Rd: radicle; Hi: hilum. Scale: 2 mm.

the remobilization of elemental nutrients during germination and early seedling development,[26] as well as to investigate the composition of biofortified and developing rice (*Oryza sativa* L.) seeds.[19,20] However, the distribution of nutrients at the tissue level remains unexplored across seeds from the Fabaceae family.

Herein, we explored a quantitative XRF approach to assess the similarity and variances of macro (K, P, S, and Ca) and micronutrients (Fe, Zn, and Mn) along with the three important legume species seeds, i.e., cowpea (*V. unguiculata* L.), kidney bean (*P. vulgaris* L.), and soybean (*G. max* L.).

2. METHODS

2.1. Sample Preparation. Seeds of cowpea (*V. unguiculata* (L.) Walp. variety BRS-Xiquexique, Brazil), kidney bean (*P. vulgaris* (L.) variety IPR Campos Gerais, Brazil), and soybean (*G. max* (L.) Merrill variety M6410 IPRO, Lagoa Bonita, Brazil) were manually cross-sectioned at the median region using a stainless-steel razor blade, preserving the embryo region. Afterward, the sampled seeds were externally and individually fixed on a 6 μm thick polypropylene film (VHG, FPPP25-R3) mounted in an X-ray sample cup (Chemplex no. 1530) for the XRF analysis. The experiments were carried out using three independent biological replicates, as detailed in Figure S1.

2.2. Space-Resolved X-ray Fluorescence Analysis. The sampled seed cross sections were measured by μ-XRF (Orbis PC EDAX). The elemental distribution of the macronutrients, i.e., sulfur (S), phosphorus (P), calcium (Ca), and potassium (K), was investigated using a 64 × 50 pixel (n = 3200 points) matrix, whereas the distribution of micronutrients, i.e., zinc (Zn), manganese (Mn), and iron (Fe), was determined throughout three 64-point line

scanning across the embryo and cotyledon regions as shown in Figure S1. Each point was investigated using a 30 μm wide X-ray beam upcoming from a 50W Rh anode operating at 20 kV and 200 μA during 2 s for the macronutrient measurements and 40 kV and 350 μA with a 25 μm thick titanium (Ti) primary filter during 10 s for the micronutrients. The analyses were performed under a vacuum atmosphere (<50 Torr), and the X-ray spectra were recorded by a silicon drift detector (SDD), with a dead time smaller than 10%.

2.3. Quantification Strategy. The concentration of macronutrients, i.e., P, S, Ca, and K, in the sampled seeds was determined using cellulose-based standards prepared with standard-grade analytical reagents (KNO$_3$, Vetec, Brazil; NaH$_2$PO$_4$·H$_2$O, Baker; Ca(NO$_3$)$_2$·4H$_2$O, Synth, Brazil; MgSO$_4$·7H$_2$O, Êxodo Científica, Brazil). The resulting 0.5 g of cellulose (cellulose binder, particle size <20 μm, Spex) pellets were then analyzed through 16-point μ-XRF linescans under the same analytical conditions employed for assessing the seeds. The calibration curves are presented in Figure S1. The trueness of the method was evaluated using certified reference materials (NIST1573a, NIST1515, NIST1547, and IAEA-V-10), and recovery values for all elements were within a 104−120% range.

Due to the inhomogeneous thickness variation across seed tissues (roughly from tenths to 3 mm), the pellet cellulose-based external calibration was not a suitable strategy for quantification of micronutrients i.e., Mn, Fe, and Zn. Particularly, the seed thickness range is under intermediate-thickness XRF condition for the latter nutrients, in which distinct thickness directly affects the nutrient X-ray fluorescence intensity and consequently their content determination. Therefore, their recorded XRF elemental intensities were herein explored.

2.4. Data Processing. Only the X-ray characteristic intensities above the instrumental limit of detection (ILOD) were considered valid. The ILOD was calculated using eq 1

$$ILOD = 3 \times \sqrt{\frac{BG}{t}} \tag{1}$$

where BG (cps) is the average of 10 random measurements of the elemental background counting rate and t (s) is the acquisition time.

The spatial correlation between the distribution of macro and micronutrients was determined through Spearman's correlation coefficient test at a 95% confidence interval, followed by a K-means clustering analysis. Besides, either the elemental concentrations or intensities recorded across each sampled seed tissue, i.e., seed coat, cotyledon, embryonal axis, and plumule, and the Krustall−Wallis analysis of variance followed by Dunn's test at a fixed 0.05 significance level were carried out. All analyses were conducted using QtiPlot (version 5.9.8, The Netherlands), RStudio (version 1.4.1106 "Tiger Daylily"; packages "*stats*" and "*ComplexHeatmap*"), and Prism (version 9.2.0) software.

3. RESULTS AND DISCUSSION

3.1. Quantitative Assessment of Macronutrient Distribution in Fabaceae Seeds. To safeguard the generation renewal of the species, seeds do exhibit unique and highly conserved structural features for enabling their proper germination and early seedling development. In eudicot species, the seeds are usually coated by layers of parenchyma and sclerenchyma cells, in which a hilum, i.e., a scar left from the seed-funiculus attachment, stands out.[27] Internally, the seed is filled up mostly by cotyledons that encompass 90% of the area, with the rest of the embryo composed of a shoot apical meristem with an already emerging leaf primordium, i.e., plumule and radicular meristem, i.e., radicle, divided by the hypocotyl axis.

Figure 1 presents the quantitative microprobe-XRF maps of P, S, K, and Ca in cowpea, soybean, and kidney bean seed cross sections. The elemental images reveal that the spatial distribution of macronutrients is heterogeneous across seed tissues but does present conserved patterns among the three Fabaceae species. Similarly, Figures S2 and S3 show that the same trends were recorded in independent biological replicates.

Regardless of the species, one should notice that both P and S were mainly found in the embryos of the seeds, encompassing the embryonal axis, i.e., hypocotyl, radicle, and plumule (Figure 1A−F). Conversely, Ca was located trapped in the seed coat and hilum (Figure 1G−I), the outermost seed tissues which play important roles in the protection of seed structural integrity and water uptake during the very first stages of the germination process.[28] Interestingly, K was distributed throughout the whole seeds, with some hotspots surrounding either embryo or seed coat tissues (Figure 1J−L).

Herein, the spatial distributions for both Ca and K recorded in cowpea, soybean, and kidney bean seeds were akin to those found in the cross sections of *C. ochroleuca* seeds,[14] another species from the Fabaceae family. Furthermore, Ca was also found mostly trapped in the tegument of rice (*O. sativa*) seeds,[29] suggesting that seeds' nutrient distribution patterns are highly conserved. However, it is important to highlight that these later studies explored a qualitative-based approach; therefore, the nutrient concentrations were not evaluated.

In this scenario, Table 1 presents the concentration of macro and micronutrients commonly found in the three species herein explored. Besides, Figure 2 presents the distribution of

Table 1. Mean Contents of P, S, K, Ca, Mn, Fe, and Zn in Soybean Seeds (*G. max*), Kidney Bean (*P. vulgaris*), and Cowpea (*V. unguiculata*)

	element	kdney bean	cowpea	soybean	reference
macronutrients ($g\ kg^{-1}$)	P	5.5	4.7	10	32−34
	S	11.6	2.4	5.4	32−34
	K	38.5	1.1	20	32, 34
	Ca	26.9	0.7	30	16, 32, 34
micronutrients ($mg\ kg^{-1}$)	Zn	27.61	45	42	16, 35
	Fe	40.6	50	71.5	33, 35, 36
	Mn	16.5	15	30	16, 35, 37

macronutrients found in the seed coat, cotyledon, embryonal axis, and plumule seed tissues and shows that the P concentration in the seeds varied from 2 to 25 g kg^{-1} (Figure 2A−D). Based on these numbers, one can conclude that most of the P remains in the embryo axis and plumule tissues, whereas a minor fraction was observed in the cotyledon. Quantification of wheat seeds found P at 72 g kg^{-1} in the aleurone layer and 40 g kg^{-1} in parts of the embryo.[30] The high phosphorus concentration in the embryo axis and plumule can be associated with different tissues located in these embryo regions, considering that the embryo axis is mostly composed of the nondifferentiated primary meristems, such as pro-cambium, ground meristem, and protodermis.[31] In addition, the intense metabolic activity in meristematic cells is related to the high amount of P in the embryo's axis and plumule cells.

Furthermore, S concentrations ranged from 1 up to ca. 12 g kg^{-1} (Figure 2E−H) and were found mainly at the plumule for the three species. The highest S contents were found in the embryo of cowpea seeds and the peripheral zone of the cotyledon in the kidney bean. The S accumulation in the cowpea plumule can be explained by its well-developed leaf primordia. The seed species can be classified considering the predominant reserve in each species; therefore, soybean is classified as an aleuro-oilseed, storing mostly lipids and proteins, whereas beans are classified as aleurone-starchy, storing mostly protein and starch.[38] Sulfur is an element related to the essential amino acids such as cysteine and methionine that are presented as globular proteins associated with the protein storage vesicles in the cotyledonary parenchyma cells.[39] In the embryo axis, S may be part of amino acid molecules or coenzymes of lipid metabolite routes and the secondary metabolism.[40]

On the other hand, Ca was herein found mostly trapped in the tegument tissues, i.e., seed coat and hilum (Figure 2I−L), in which concentrations ranged from 1 up to 50 mg kg^{-1}. The high Ca concentration in the tegument might be associated with the presence of a pectin-rich cell wall, mainly composed of Ca pectate, a Ca binding to nonmethyl esterified homo-galacturonan that affects the stiffness of the wall.[41] As the outermost tissues, both seed coat and hilum play crucial roles in protecting the seeds and modulating their interactions with the surrounding environment, e.g., water absorption that triggers the germination process.[28] Moreover, Ca is also located at plant cell vacuoles as prismatic crystals of Ca oxalate[42] but at a lower concentration. Besides, the μ-XRF analysis demonstrated that Ca was also accumulated in the
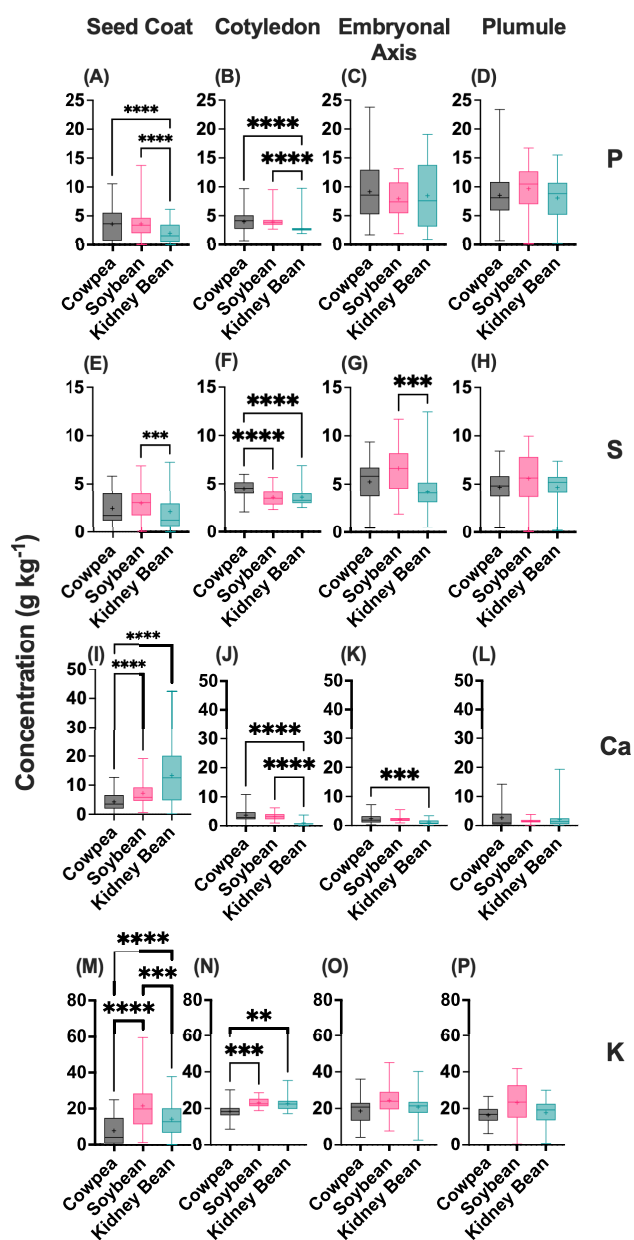
Figure 2. Boxplots of phosphorus (A−D), sulfur (E−H), calcium (I−L), and potassium (M−P) concentrations recorded at the seed coat, cotyledon, embryonal axis, and plumule tissues of cowpea, soybean, and kidney bean seed cross sections. Data derived from three independent biological replications and were subjected to Krustall−Wallis's analysis of variance followed by Dunn's test at a fixed 0.05 significance level. (+) Mean values; (*) $p < 0.05$; (**) $p < 0.01$; (***, ****) $p < 0.001$.

three studied species in the hilar region, similar to the results recorded for soybean in a previous XRF-based study.[26]

Until now, the role of Ca at the hilum is not completely understood. Considering that the water enters majorly through the hilum during the imbibition process, it is not clear whether the Ca deposited at the hilum can be remobilized to the embryo and then induce embryo germination.

Conversely, the K concentration ranged from 1 to 52 g kg^{-1} in cowpea and varied from 1 to ca. 90 g kg^{-1} in kidney bean and soybean seeds (Figure 2M−P). Potassium plays an important role in homeostasis of osmotic potential and ergastic

substance biosynthesis, such as carbohydrates, as well as ensuring protein stability.[43] Besides, it was also verified that K is easily remobilized from the cotyledonary parenchyma cells to the embryo axis as the primary roots emerge during hypocotyl elongation of the germination process of soybean seeds.[26]

Furthermore, one should keep in mind that the nutrient content in the seed might be related to its vigor. For example, Cotrim et al. found a positive correlation between the vigor and P, S, K, and Ca contents along the embryonic axis of the *C. ochroleuca* seeds.[14] Then, the nutrient monitoring in seeds might also be explored as a strategy for evaluating their vigor.

3.2. Qualitative Assessment of Micronutrient Distribution in Fabaceae Seeds. For evaluating the spatial distribution of micronutrients in seeds, the linescan analysis approach showed to be more adequate than the maps, since the lower number of probed points enables exploring longer measurement time, thereby increasing the signal-to-noise ratio and the detection of trace elements, such as Mn, Fe, and Zn in vegetal samples.[16,44−46] In this regard, a triple series of 64-point linescans were performed for each triplicate of Fabaceae seeds. Figure S4 details the linescans performed on seeds, while Figures S5−S7 show the XRF signals detected for Mn, Fe, and Zn in each one of the probed points.

Figure 3 presents the distribution of Mn, Fe, and Zn recorded in the seed coat, cotyledon, embryonal axis, and plumule seed tissues. It reveals that Mn presented lower XRF intensities compared to Fe and Zn, with the Mn values found in the cotyledon and embryonal axis tissues of soybean seeds (Figure 3A−D). Moreover, the Fe intensities were the highest among the micronutrients and also found mostly concentrated within the embryo axis. Aside from the embryo axis, a similar Fe concentration content was found in the cotyledon of all seed species (Figure 3E−H). Finally, the highest Zn XRF intensities were found in each bean-type embryo axis. Note that no statistically significant difference was found between the concentration of Zn in the seed coat and embryo among the beans (Figure 3I−L). On the other hand, Zn concentrations in the cotyledon and plumule were similar among the three species.

Synchrotron-based XRF maps of *A. thaliana* showed a slightly higher Zn concentration of Zn in the cotyledon tissue compared to the radicle one.[15] In addition, as a cofactor for several enzymes related to gene expression, e.g., the Zn-finger transcriptional factor, the high amount of Zn found at the embryo axis and plumule might likely be associated with its role during seed germination and early development.

Furthermore, space-resolved microchemical maps of germinating rice grain cross sections showed that Mn can be accumulated in the seed coat and scutellum and then translocated to the leaf primordium.[47] Manganese participates in the metalloenzyme cluster of the oxygen-evolving complex in photosystem II, and it acts as a cofactor for several enzymes related to the secondary metabolism and as enzymes that are associated with the detoxification process. Oxalate oxidase, for instance, is an Mn-dependent[48] highly expressed during the embryo germination of wheat and likely plays an important role in the protection against oxidative stresses during seed maturation and germination.[49] In addition, Mn is also related to the formation of lignin that forms the cell wall.[50]

Due to the low-energy X-ray fluorescence absorption by the X-ray detector window and the low fluorescence yield, some lower atomic number macronutrients, e.g., B, Mg, and N, were
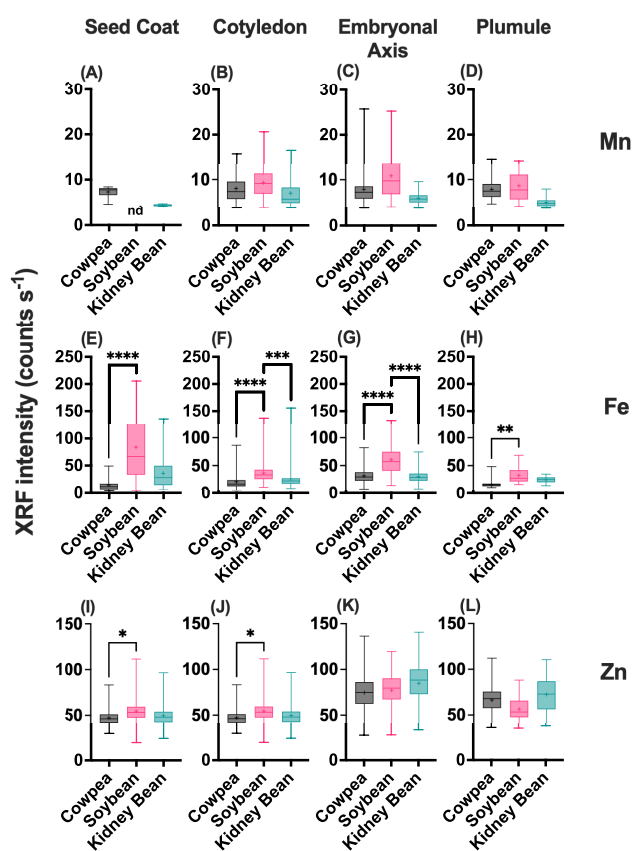
Figure 3. Boxplots of manganese (A–D), iron (E–H), and zinc (I–L) XRF elemental intensities recorded at the seed coat, cotyledon, embryonal axis, and plumule tissues of cowpea, soybean, and kidney bean seed cross sections. Data derived from three independent biological replications and were subjected to Krustall–Wallis's analysis of variance followed by Dunn's test at a fixed 0.05 significance level. (+) Mean values; (*) $p < 0.05$; (**) $p < 0.01$; (***, ****) $p < 0.001$.

not detected. Additionally, the detection of some micronutrients, such as Cu and Mo, was not possible under the current instrumental conditions due to their lower concentration.

3.3. Tissue-Resolved Correlation of Nutrient Distribution in Fabaceae Seeds. Aiming at understanding the

spatial distribution patterns displayed by the probed elements across the Fabaceae seeds, Figure 4 presents the heatmaps of Spearman's correlation coefficients determined across cowpea, soybean, and kidney bean seeds with XRF recorded values.

For the macronutrients (Figure 4A), it reveals that the highest correlations were observed between P and S, S and K. Conversely, Ca presented the lowest correlations in the three Fabaceae, showing lower correlations with K in cowpea, both K and P in the kidney bean ones, and with S in soybean seeds. These results follow a similar trend as those observed in developing soybean seeds.[26] For the micronutrients (Figure 4B), higher correlation values were usually recorded compared to the macronutrient ones. An interesting association between Fe and Mn, and Fe and Zn was observed in cowpea and soybean seeds, respectively. A similar association between Mn, Fe, and Zn was observed in the *Turkish pea*.[51]

Furthermore, the *K*-means clustering also revealed that regardless of macro and micronutrients, the elemental distribution of kidney bean and soybean and soybean seeds was more related compared to those of the cowpea ones.

4. CONCLUSIONS

The present approach unveils the feasibility of X-ray fluorescence spectroscopy to depict the elemental distribution of seeds and unveils that the nutrients are not homogeneously distributed in Fabaceae seeds but follow similar trends. Sulfur and P concentrated mostly in the seed's embryo, whereas Ca was mostly in the seed coat and hilum, and K presented a more homogenous distribution throughout the seeds. Besides, Zn and Mn seem to share similar locations mainly throughout the embryo. These results improve the understanding of the nutrient composition of seeds and might shed light on the understanding of their roles in seed physiology. This current approach might be useful for helping in the development of nutritional strategies that might improve seed vigor and the performance of their upcoming plants in the field.

■ ASSOCIATED CONTENT

⑤ Supporting Information

The Supporting Information is available free of charge at https://pubs.acs.org/doi/10.1021/acsagscitech.2c00260.

> Calibration curves derived from cellulose-based standards for P, S, Ca, and K, respectively (Figure S1); independent replicates of the quantitative XRF maps
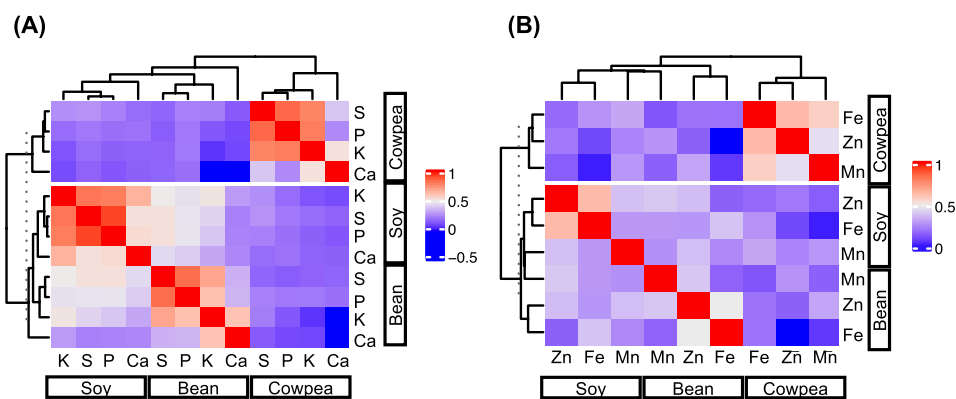

Figure 4. Heatmaps of Spearman's correlation coefficient for XRF-probed macro (A) and micronutrients (B) spatial distribution across cowpea, soybean, and kidney bean cross sections. The *K*-means clustering displays the similarity of the correlation values found for each seed species assessed.

revealing the distribution of P, S, Ca, and K in cowpea, soybean, and kidney bean seed cross sections (Figures S2 and S3); photographs and representation of each line scanned through XRF to assess the distribution of Mn, Fe, and Zn across the tissues of cowpea, soybean, and kidney bean seed cross sections (Figure S4), as shown in the independent replicates (Figures S5−S7) (PDF)

■ AUTHOR INFORMATION

Corresponding Author

Hudson Wallace Pereira de Carvalho − Centre for Nuclear Energy in Agriculture, University of São Paulo, Piracicaba 13416-000, Brazil; ◉ orcid.org/0000-0003-0875-3261; Email: hudson@cena.usp.br

Authors

Gabriel Sgarbiero Montanha − Centre for Nuclear Energy in Agriculture, University of São Paulo, Piracicaba 13416-000, Brazil; Biology and Biotechnology Department "Charles Darwin", Sapienza University of Rome, Rome 00185, Italy; ◉ orcid.org/0000-0003-1375-2351

Sara Luiza Zachi Romeu − Centre for Nuclear Energy in Agriculture, University of São Paulo, Piracicaba 13416-000, Brazil

João Paulo Rodrigues Marques − Department of Basic Sciences, Faculty of Animal Science and Food Engineering, University of São Paulo, Pirassununga 13635-900, Brazil

Lívia Araújo Rohr − Laboratory of Seed Analysis, Luiz de Queiroz College of Agriculture, University of São Paulo, Piracicaba 13418-900, Brazil

Eduardo de Almeida − Centre for Nuclear Energy in Agriculture, University of São Paulo, Piracicaba 13416-000, Brazil

André Rodrigues dos Reis − Department of Biosystems Engineering, Faculty of Science and Engineering, São Paulo State University, Tupã 17602-496, Brazil; ◉ orcid.org/0000-0002-6527-2520

Francisco Scaglia Linhares − Centre for Nuclear Energy in Agriculture, University of São Paulo, Piracicaba 13416-000, Brazil

Sabrina Sabatini − Biology and Biotechnology Department "Charles Darwin", Sapienza University of Rome, Rome 00185, Italy

Complete contact information is available at:
https://pubs.acs.org/10.1021/acsagscitech.2c00260

Author Contributions

H.W.P.d.C., J.P.R.M., and G.S.M.: Conceptualization; H.W.P.d.C., S.L.Z.R., and G.S.M.: methodology; H.W.P.d.C.: resources; G.S.M, S.L.Z.R., and H.W.P.d.C.: data curation; G.S.M., S.L.Z.R., E.d.A., L.A.R., J.P.R.M., and H.W.P.d.C.: original draft preparation; and S.L.Z.R., G.S.M., E.d.A., L.A.R., J.P.R.M., F.S.L., and H.W.P.d.C.: review and editing.

Notes

The authors declare no competing financial interest.
The data underlying this article will be shared on reasonable request to the corresponding author.

■ ACKNOWLEDGMENTS

■ REFERENCES

(1) Stagnari, F.; Maggio, A.; Galieni, A.; Pisante, M. Multiple benefits of legumes for agriculture sustainability: an overview. Chem. Biol. Technol. Agric. 2017, 4, 2.

(2) Kenicer, G. Legumes of the World. Edinb. J. Bot. 2005, 62, 195−196.

(3) Hartman, G. L.; West, E. D.; Herman, T. K. Crops that feed the World 2. Soybean—worldwide production, use, and constraints caused by pathogens and pests. Food Secur. 2011, 3, 5−17.

(4) Copeland, L. O.; McDonald, M. B.Principles of Seed Science and Technology, 1st ed.; Springer: New York, 2001.

(5) American Soybean Association. Soystats 2022: A Reference Guide to Imprtant Soybean Facts & Figures, 2022.

(6) Milberg, P. E. R.; Lamont, B. B. Seed/cotyledon size and nutrient content play a major role in early performance of species on nutrient-poor soils. New Phytol. 1997, 137, 665−672.

(7) Johnson, T. R.; Kane, M. E.; Pérez, H. E. Examining the interaction of light, nutrients and carbohydrates on seed germination and early seedling development of Bletia purpurea (Orchidaceae). Plant Growth Regul. 2011, 63, 89−99.

(8) Bewley, J. D.; Bradford, K. J.; Hilhorst, H. W. M.et al.Seeds; Springer: New York, 2013.

(9) Ghaderi-Far, F.; Gherekhloo, J.; Alimagham, M. Influence of environmental factors on seed germination and seedling emergence of yellow sweet clover (Melilotus officinalis). Planta Daninha 2010, 28, 463−469.

(10) Lamichhane, J. R.; Debaeke, P.; Steinberg, C.; et al. Abiotic and biotic factors affecting crop seed germination and seedling emergence: a conceptual framework. Plant Soil 2018, 432, 1−28.

(11) Bonilla, I.; El-Hamdaoui, A.; Bolaños, L. Boron and calcium increasePisum sativum seed germination and seedling development under salt stress. Plant Soil 2004, 267, 97−107.

(12) Martínez-Ballesta, M. C.; Egea-Gilabert, C.; Conesa, E.; et al. The Importance of Ion Homeostasis and Nutrient Status in Seed Development and Germination. Agronomy 2020, 10, 504.

(13) Osuna, D.; Prieto, P.; Aguilar, M. Control of Seed Germination and Plant Development by Carbon and Nitrogen Availability. Front. Plant Sci. 2015, 6, 1023.

(14) Cotrim, M. F.; da Silva, J. B.; dos Santos Lourenço, F. M.; et al. Studying the link between physiological performance of Crotalaria ochroleuca and the distribution of Ca, P, K and S in seeds with X-ray fluorescence. PLoS One 2019, 14, e0222987.

(15) Young, L.; Westcott, N.; Christensen, C.; et al. Inferring the geometry of fourth-period metallic elements in Arabidopsis thaliana seeds using synchrotron-based multi-angle X-ray fluorescence mapping. Ann. Bot. 2007, 100, 1357−1365.

(16) Lanza, M. G. D. B.; Silva, V. M.; Montanha, G. S.; et al. Assessment of selenium spatial distribution using μ-XFR in cowpea (Vigna unguiculata (L.) Walp.) plants: Integration of physiological and biochemical responses. Ecotoxicol. Environ. Saf. 2021, 207, No. 111216.

(17) Malan, H. L.; Mesjasz-Przybylowicz, J.; Przybylowicz, W. J.; et al. Distribution patterns of the metal pollutants Cd and Ni in soybean seeds. Nucl. Instrum. Methods Phys. Res. B 2012, 273, 157−160.

(18) Jiang, Y.; Mehdawi, A. F.; et al. Characterization of Selenium Accumulation, Localization and Speciation in Buckwheat—Implications for Biofortification. Front. Plant Sci. 2018, 9, No. 1583.

(19) dos Reis, A. R.; Boleta, E. H. M.; Alves, C. Z.; et al. Selenium toxicity in upland field-grown rice: Seed physiology responses and nutrient distribution using the μ-XRF technique. Ecotoxicol. Environ. Saf. 2020, 190, No. 110147.

(20) Iwai, T.; Takahashi, M.; Oda, K.; et al. Dynamic changes in the distribution of minerals in relation to phytic acid accumulation during rice seed development. *Plant Physiol.* **2012**, *160*, 2007−2014.

(21) Savassa, S. M.; Castillo-Michel, H.; Pradas del Real, A. E.; et al. Ag nanoparticles enhancing Phaseolus vulgaris seedling development: understanding nanoparticle migration and chemical transformation across the seed coat. *Environ. Sci.: Nano* **2021**, *8*, 493−501.

(22) de Almeida, E.; Montanha, G. S.; Pereira de Carvalho, H. W.; Marguí, E. Evaluation of energy dispersive X-ray fluorescence and total reflection X-ray fluorescence spectrometry for vegetal mass-limited sample analysis: Application to soybean root and shoots. *Spectrochim. Acta, Part B* **2020**, *170*, No. 105915.

(23) Longnecker, N. E.; Robson, A. D.*Distribution and Transport of Zinc in Plants BT − Zinc in Soils and Plants*; Proceedings of the International Symposium on "Zinc in Soils and Plants", University of Western Australia, 27−28 September, 1993; pp 79−91.

(24) de Brier, N.; Gomand, S.; Donner, E.; et al. Element distribution and iron speciation in mature wheat grains (*Triticum aestivum* L.) using synchrotron X-ray fluorescence microscopy mapping and X-ray absorption near-edge structure (XANES) imaging. *Plant, Cell Environ.* **2016**, *39*, 1835−1847.

(25) Rodrigues, E. S.; Gomes, M. H. F.; Duran, N. M.; et al. Laboratory Microprobe X-Ray Fluorescence in Plant Science: Emerging Applications and Case Studies. *Front. Plant Sci.* **2018**, *9*, 1588.

(26) Romeu, S. L. Z.; Marques, J. P. R.; Montanha, G. S.; et al. Chemometrics unraveling nutrient dynamics during soybean seed germination. *Microchem. J.* **2021**, *164*, No. 106045.

(27) Murley, M. R. Seeds of the Cruciferae of Northeastern North America. *Am. Midl. Nat.* **1951**, *46*, 1−81.

(28) Souza, F. H. D. D.; Dübbern Marcos-Filho, J. The seed coat as a modulator of seed-environment relationships in Fabaceae. *Braz. J. Bot.* **2001**, *24*, 365−375.

(29) Lu, L.; Tian, S.; Liao, H.; et al. Analysis of Metal Element Distributions in Rice (Oryza sativa L.) Seeds and Relocation during Germination Based on X-Ray Fluorescence Imaging of Zn, Fe, K, Ca, and Mn. *PLoS One* **2013**, *8*, No. e57360.

(30) Singh, S. P.; Vogel-Mikuš, K.; Arčon, I.; et al. Pattern of iron distribution in maternal and filial tissues in wheat grains with contrasting levels of iron. *J. Exp. Bot.* **2013**, *64*, 3249−3260.

(31) Bewley, J. D.; Bradford, K. J.; Hilhorst, H. W. M.et al.*Structure and Composition BT − Seeds: Physiology of Development, Germination and Dormancy*, 3rd ed.; Springer: New York, 2013; pp 1−25.

(32) Kachinski, W. D.; Ávila, F. W.; Muller, M. M. L.; et al. Nutrition, yield and nutrient export in common bean under zinc fertilization in no-till system. *Ciência Agrotecnol.* **2020**, *44*, 44.

(33) Silva, V. M.; Boleta, E. H.; Martins, J. T.; et al. Agronomic biofortification of cowpea with selenium: effects of selenate and selenite applications on selenium and phytate concentrations in seeds. *J. Sci. Food Agric.* **2019**, *99*, 5969−5983.

(34) Seixas, C. D. S.; Neumaier, N.; Balbinot Junior, A. A.et al.*Tecnologias de Produção de Soja*Embrapa Soja: Londrina; 2020.

(35) Grela, E. R.; Samolińska, W.; Kiczorowska, B.; et al. Content of Minerals and Fatty Acids and Their Correlation with Phytochemical Compounds and Antioxidant Activity of Leguminous Seeds. *Biol. Trace Elem. Res.* **2017**, *180*, 338−348.

(36) Bellaloui, N.; Bruns, H. A.; Gillen Anne, M.; et al. Soybean seed protein, oil, fatty acids, and mineral composition as influenced by soybean-corn rotation. *Agric. Sci.* **2010**, *01*, 102−109.

(37) de Vargas, R. L.; Schuch, L. O. B.; Barros, W. S.; et al. Macronutrients and Micronutrients Variability in Soybean Seeds. *J. Agric. Sci.* **2018**, *10*, 209.

(38) Marcos-Filho, J.*Seed Physiology of Cultivated Plants*; ABRATES: Londrina, 2016.

(39) Krishnan, H. B.; Kim, W-S.; Oehrle, N. W.; et al. Effect of Heat Stress on Seed Protein Composition and Ultrastructure of Protein Storage Vacuoles in the Cotyledonary Parenchyma Cells of Soybean Genotypes That Are Either Tolerant or Sensitive to Elevated Temperatures. *Int. J. Mol. Sci.* **2020**, *21*, 4775.

(40) Becana, M.; Wienkoop, S.; Matamoros, M. A. Sulfur Transport and Metabolism in Legume Root Nodules. *Front. Plant Sci.* **2018**, *9*, 1434.

(41) Caffall, K. H.; Mohnen, D. The structure, function, and biosynthesis of plant cell wall pectic polysaccharides. *Carbohydr. Res.* **2009**, *344*, 1879−1900.

(42) Ilarslan, H.; Palmer, R. G.; Horner, H. T. Calcium Oxalate Crystals in Developing Seeds of Soybean. *Ann. Bot.* **2001**, *88*, 243−257.

(43) Malavolta, E.*Manual de Nutrição Mineral de Plantas*; Agronômica Ceres: São Paulo, 2006.

(44) Mijovilovich, A.; Morina, F.; Bokhari, S. N.; et al. Analysis of trace metal distribution in plants with lab-based microscopic X-ray fluorescence imaging. *Plant Methods* **2020**, *16*, 82.

(45) Montanha, G. S.; Rodrigues, E. S.; Marques, JPR.; et al. X-ray fluorescence spectroscopy (XRF) applied to plant science: challenges towards in vivo analysis of plants. *Metallomics* **2020**, *12*, 183−192.

(46) Gonzalez, J.; Simões, G.; Bernini, R.; et al. Elemental Concentration and Sulfur Chemical Speciation in the Amazonian Plant Andira surinamensis Using Synchrotron Radiation Techniques (SR-XRF, XANES), RBS and WD-XRF. *J. Braz. Chem. Soc.* **2019**, *30*, 1887−1896.

(47) Takahashi, M.; Nozoye, T.; Kitajima, N.; et al. In vivo analysis of metal distribution and expression of metal transporters in rice seed during germination process by microarray and X-ray Fluorescence Imaging of Fe, Zn, Mn, and Cu. *Plant Soil* **2009**, *325*, 39−51.

(48) Alejandro, S.; Höller, S.; Meier, B.; Peiter, E. Manganese in Plants: From Acquisition to Subcellular Allocation. *Front. Plant Sci.* **2020**, *11*, 300.

(49) Caliskan, M.; Turet, M.; Cuming, A. C. Formation of wheat (Triticum aestivum L.) embryogenic callus involves peroxide-generating germin-like oxalate oxidase. *Planta* **2004**, *219*, 132−140.

(50) Kirkby, E.*Introduction, Definition and Classification of Nutrients*. In *Marschner PBT-MMN of HP*, 3rd ed.; Academic Press: San Diego, 2012; Chapter 1, pp 3−5.

(51) Demirbas, A. Micro and macronutrients diversity in Turkish pea (Pisum sativum) Germplasm. *Int. J. Agric. Biol.* **2018**, *20*, 701−710.